

Hydrothermal Synthesis, Crystal Structure, and Magnetic Properties of a New Inorganic Vanadium(III) Phosphate with a Chain Structure

Stanislav Ferdov,^{†,‡,§,⊥} Mario S. Reis,[‡] Zhi Lin,^{*,†} and Rute A. Sá Ferreira[‡]

Departments of Chemistry and Physics, CICECO, University of Aveiro, 3810-193 Aveiro, Portugal, and Department of Physics, University of Minho, Guimarães, Portugal

Received July 15, 2008

A new vanadium(III) phosphate, $\text{Na}_3\text{V}(\text{OH})(\text{HPO}_4)(\text{PO}_4)$, has been synthesized by using mild hydrothermal conditions under autogeneous pressure. This material represents a very rare example of sodium vanadium(III) phosphate with a chain structure. The crystal structure has been determined by refinement of powder X-ray diffraction data, starting from the atomic coordinates of an isotopic compound, $\text{Na}_3\text{Al}(\text{OH})(\text{HPO}_4)(\text{PO}_4)$, which was obtained under high temperature and high pressure. The phase crystallizes in monoclinic space group $C2/m$ (No. 12) with lattice parameters $a = 15.423(9) \text{ \AA}$, $b = 7.280(0) \text{ \AA}$, $c = 7.070(9) \text{ \AA}$, $\beta = 96.79(7)^\circ$, $V = 788.3(9) \text{ \AA}^3$, and $Z = 4$. The structure consists of one-dimensional chains composed of corner-sharing $\text{VO}_5(\text{OH})$ octahedra running along the b direction. They are decorated by isolated PO_4 and HPO_4 tetrahedra sharing two of their corners with the ones of the vanadium octahedra. The interconnection between the chains is assured by three crystallographically distinct Na^+ cations. Magnetic investigation confirms the 3+ oxidation state of the vanadium ions and reveals an antiferromagnetic arrangement between those ions through the chain.

1. Introduction

Vanadium phosphates exist in a wide range of structural forms because of their variable oxidation states as well as the large diversity in the bonding of the VO_n polyhedra (tetrahedra, square pyramids, and distorted and regular octahedra) and the PO_4 tetrahedra. The association of different vanadium oxidation states (V, IV, and III) with their various polyhedra leads to a large diversity of the resulting structures and properties.¹ The major interest in vanadium phosphates originates from the catalytic applications of vanadyl pyrophosphate in the selective oxidation of butane to maleic anhydride.^{1–3} Vanadium phosphates have also shown promising results as heterogeneous catalysts in the selective oxidation of propane to acrylic acid and of pentane to maleic and phthalic anhydride and in the oxidative

dehydrogenation of ethane, propane, etc.⁴ In this respect, some of the most widely studied are the vanadium(V) vanadyl orthophosphates (α -, β -, γ -, δ -, and ω - VOPO_4 and $\text{VOPO}_4 \cdot 2\text{H}_2\text{O}$) and the vanadium(IV) vanadyl hydrogen phosphates ($\text{VOHPO}_4 \cdot 2\text{H}_2\text{O}$, $\text{VOHPO}_4 \cdot 0.5\text{H}_2\text{O}$ and $\text{VO}(\text{H}_2\text{PO}_4)_2$), vanadyl metaphosphate ($\text{VO}(\text{PO}_3)_2$), and vanadyl pyrophosphate ($(\text{VO})_2\text{P}_2\text{O}_7$), claimed to be an active phase of commercial catalysts.^{4–8} Additionally, reduced vanadium phosphate systems with low-dimensional structures often exhibit unusual magnetic behavior, which makes them very attractive for magnetic and electrochemical studies.^{9–11} Boudin et al. have reviewed 126 vanadium phosphate compounds with mono- or divalent metallic cations. The

* To whom correspondence should be addressed. E-mail: zlin@ua.pt. Tel: 351 234401519. Fax: 351 234370084.

[†] Department of Chemistry, CICECO, University of Aveiro.

[‡] Department of Physics, CICECO, University of Aveiro.

[§] University of Minho.

[⊥] On leave from the Central Laboratory of Mineralogy and Crystallography, Bulgarian Academy of Sciences.

(1) Cheetham, A. K.; Ferey, G.; Loiseau, T. *Angew. Chem., Int. Ed.* **1999**, *38*, 3268.

(2) Seeboth, H.; Kubias, B.; Wolf, H.; Luche, B. *Chem. Technol.* **1976**, *28*, 730.

(3) Bordes, E.; Courtine, P. *J. Chem. Soc., Chem. Commun.* **1985**, 294.

(4) Centi, G. *Catal. Today* **1993**, *16*, 1.

(5) Bordes, E. *Catal. Today* **1987**, *1*, 499.

(6) Abdelouahab, F. B.; Olier, R.; Guilhaume, N.; Lefebvre, F.; Volta, J. C. *J. Catal.* **1992**, *134*, 151.

(7) Hutchings, G. J.; Sananes, M. T.; Sajip, S.; Kiely, Ch. J.; Burrows, A.; Ellison, I. J.; Volta, J. C. *Catal. Today* **1997**, *33*, 161.

(8) Gulians, V. V.; Benziger, J. B.; Sundaresan, S.; Wachs, I. E.; Jehng, J.-M.; Roberts, J. E. *Catal. Today* **1996**, *28*, 275.

(9) Panin, R. V.; Shpanchenko, R. V.; Mironov, A. V.; Velikodny, Yu. A.; Antipov, E. V.; Hadermann, J.; Tarnopolsky, V. A.; Yaroslavtsev, A. B.; Kaul, E. E.; Geibel, C. *Chem. Mater.* **2004**, *16*, 1048.

(10) Alda, E.; Bazán, B.; Mesa, J. L.; Pizarro, J. L.; Arriortua, M. I.; Rojo, T. *J. Solid State Chem.* **2003**, *173*, 101.

(11) Whittingham, M. S.; Song, Y.; Lutta, S.; Zavalij, P. Y.; Chernova, N. A. *J. Mater. Chem.* **2005**, *15*, 3362.

vanadium ion in one third of these phosphates exists in oxidation state 3+. The magnetic and catalytic properties of 45 and 15 compounds, respectively, are reviewed, and their structure–property relationships are also discussed.¹² However, the preparation of new alkaline vanadium(III) phosphates is still possible.

Here, we report the mild hydrothermal synthesis and structural and magnetic characterization of a new rare inorganic vanadium(III) phosphate with a chain structure. This is the second inorganic metal phosphate synthesized via using 2-methylpentamethylenediamine (MPMD),¹³ and to the best of our knowledge, it is the first sodium vanadium(III) phosphate containing isolated chains of vanadium polyhedra.

2. Experimental Section

2.1. Synthesis. In a typical synthesis of $\text{Na}_3\text{V}(\text{OH})(\text{HPO}_4)(\text{PO}_4)$, a solution of 0.72 g of sodium dihydrogen phosphate— NaH_2PO_4 (Aldrich) and 10.01 g of distilled water was mixed with 10.2 g of MPMD (DuPont). Then, 0.11 g of vanadium(IV) oxide sulfate pentahydrate ($\text{VOSO}_4 \cdot 5\text{H}_2\text{O}$, Riedel-de Haën) was dissolved in 4.65 g of distilled water and added to the above solution. The resulting mixture was homogenized for 40 min and then transferred into a Teflon-lined autoclave (45 mL). The crystallization was performed under static conditions at 150 °C for 7 days. After fast cooling with flowing water, the run product was filtered with distilled water and dried at 40 °C for 1 day. The phase crystallizes as 40–70 μm aggregates composed of prismatic particles (Figure S1 in the Supporting Information). Similar to a previously reported material,¹³ to date, $\text{Na}_3\text{V}(\text{OH})(\text{HPO}_4)(\text{PO}_4)$ must be prepared with MPMD in the starting mixture, although this amine is not included in the structure (see infrared data). The mass loss before 475 °C (Figure S2 in the Supporting Information) is mainly due to decomposition of the title compound, which also suggests the absence of amine. This implies its role as a reactant for achieving proper conditions for crystallization. The preparation of $\text{Na}_3\text{V}(\text{OH})(\text{HPO}_4)(\text{PO}_4)$ appeared to be quite sensitive toward the grade of the reactants used in the initial batch. For instance, in the same system and conditions, when the source of NaH_2PO_4 is substituted by sodium phosphate dibasic dodecahydrate— $\text{Na}_2\text{HPO}_4 \cdot 12\text{H}_2\text{O}$ (Aldrich), we get vanadium(IV) phosphate with a cubic structure, $\text{Na}_{3.053}(\text{V}_5\text{O}_9)(\text{PO}_4)_2(\text{OH})_{0.1}(\text{H}_2\text{O})_8$.¹⁴

2.2. Characterization. The scanning electron microscopy (SEM) images and chemical analysis (EDS) were carried out using a Hitachi S-4100 scanning electron microscope equipped with a Römteck EDS system. Powder X-ray diffraction (XRD) data were collected on a Philips X'Pert MPD diffractometer (Cu $K\alpha_{1,2}$ X-radiation) using a fixed divergence slit of 0.25° and a flat-plate sample holder in a Bragg–Brentano parafocusing optics configuration. The diffraction intensity was collected by the step scan method (step 0.02° and time 420 s) in the 2θ range between 10 and 90°. Fourier transform infrared spectra (FTIR) of powdered samples suspended in KBr pellets were acquired between 400 and 4000 cm^{-1} using a Mattson model 7000 spectrometer, resolution 2 cm^{-1} . The thermogravimetric (TG) curve was measured with a TG-50 Shimadzu analyzer. The samples were heated under air at a rate

of 5 °C/min. Direct current (dc) magnetic susceptibility (χ_{dc}) was measured in a VSM magnetometer, from 50 K up to 250 K, under a magnetic field of 5 kOe.

3. Results and Discussion

3.1. Structure Refinement. The powder XRD pattern of $\text{Na}_3\text{V}(\text{OH})(\text{HPO}_4)(\text{PO}_4)$ was indexed from 19 accurately measured reflection positions by using the *TREOR* program.¹⁵ A monoclinic cell was obtained, $a = 15.413(9)$ Å, $b = 7.275(0)$ Å, $c = 7.067(6)$ Å, and $\beta = 96.78(3)^\circ$, giving the figures of merit $M_{19} = 47.6$ ¹⁶ and $F_{19} = 80.5$ (0.0044, 54).¹⁷ No additional systematic absences from the expected ones for space group (*C2/m*) were observed. These data were used for searching in the available structural databases (ICDD, International Centre for Diffraction Data, and ICSD, Inorganic Crystal Structure Database), which indicated a similarity between the present phase and $\text{Na}_3(\text{M})(\text{OH})(\text{HPO}_4)(\text{PO}_4)$ ($\text{M} = \text{Al}, \text{Ga}$).¹⁸ Using this information, the structural elucidation was performed by the Rietveld method with the *TOPAS-3* package¹⁹ and starting from the atomic coordinates of the $\text{Na}_3\text{Al}(\text{OH})(\text{HPO}_4)(\text{PO}_4)$ isostructural compound.¹⁸ After extraction of structure factor amplitudes by the Le Bail method,²⁰ the initial structural refinement cycles included the scale factor, the zero-point shift, the lattice parameters, and the background parameters as variables. Following satisfactory matching of the peak positions, the atomic positions, the thermal parameters, and the peak profile parameters including the peak asymmetry were refined. All of the atoms were refined with individual isotropic displacement parameters. The higher values of Na(3) and P(2) could be due to the poor crystallinity of the sample together with possible disorder over these positions.

The final Rietveld plot is shown in Figure 1. Details of the final refinement and atomic parameters are given in Tables 1 and 2. Selected bond distances and bond valence sum (BVS) calculations are listed in Table 3. Bond angles are given in Table S1 in the Supporting Information. The chemical analysis data by energy-dispersive X-ray spectrometry (EDS) obtained from a number of different particles Na: P:V (3.0:2.07:1.11) are in fair agreement with the values obtained from the structural characterization Na:P:V (3.0:2.0:1.0).

3.2. Structure Description. The crystal structure consists of one-dimensional chains composed of corner-sharing $\text{VO}_5(\text{OH})$ octahedra running along the b direction (Figure 2a). They are separated by isolated PO_4 and HPO_4 tetrahedra sharing two of their corners with the ones of the vanadium octahedra. The interconnection between the chains is assured by three crystallographically distinct Na^+ cations (Figure 2b).

(12) Boudin, S.; Guesdon, A.; Leclaire, A.; Borel, M.-M. *Int. J. Inorg. Mater.* **2000**, *2*, 561.

(13) Ferdov, S.; Lopes, A. M. L.; Lin, Z.; Ferreira, R. A. S. *Chem. Mater.* **2007**, *19*, 6025.

(14) Schindler, M.; Joswig, W.; Baur, W. H. *Z. Anorg. Allg. Chem.* **1997**, *623*, 45.

(15) Werner, P. E.; Eriksson, L.; Westdahl, M. *J. Appl. Crystallogr.* **1985**, *18*, 367.

(16) de Wolf, P. M. *J. Appl. Crystallogr.* **1968**, *1*, 108.

(17) Smith, G. S.; Snyder, R. L. *Appl. Crystallogr.* **1979**, *12*, 60.

(18) Lii, K.-H.; Wang, S.-L. *J. Solid State Chem.* **1997**, *128*, 21.

(19) *TOPAS V3.0: General profile and structure analysis software for powder diffraction data*; Bruker AXS: Karlsruhe, Germany.

(20) Le Bail, A.; Duroy, H.; Fourquet, J. L. *Mater. Res. Bull.* **1988**, *23*, 447.

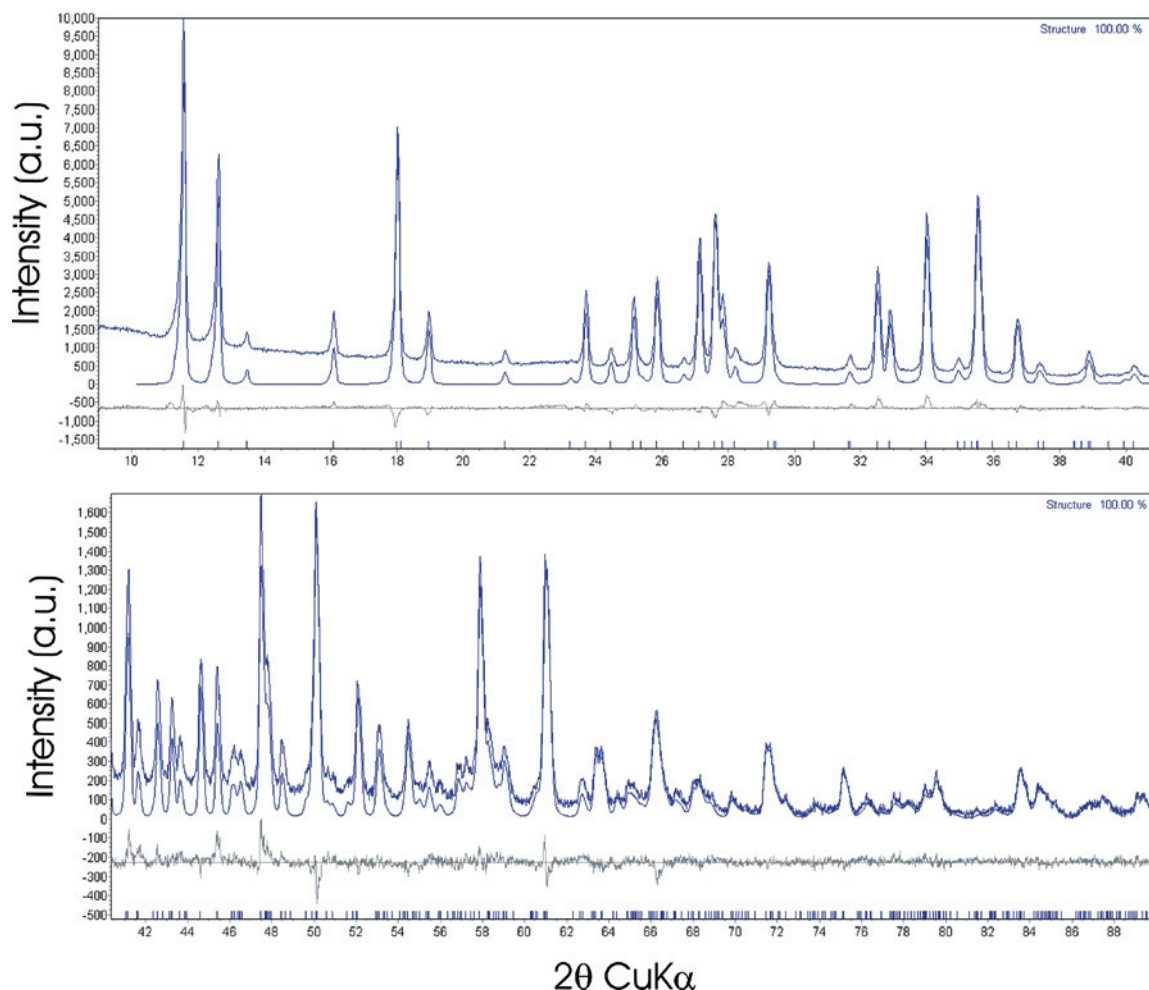


Figure 1. Experimental (upper line) and simulated (bottom line) powder XRD patterns of $\text{Na}_3\text{V}(\text{OH})(\text{HPO}_4)(\text{PO}_4)$.

Table 1. Crystal Data and Structure Refinement Parameters

compound	$\text{Na}_3\text{V}(\text{OH})(\text{HPO}_4)(\text{PO}_4)$
chemical formula	$\text{Na}_3\text{VP}_2\text{O}_9\text{H}_2$
fw	1303.41 g/mol
cryst syst	monoclinic
space group	$C2/m$ (No. 12)
unit cell dimens	$a = 15.423(9)$ Å, $b = 7.280(0)$ Å, $c = 7.070(9)$ Å, $\beta = 96.79(7)^\circ$
volume	$788.3(9)$ Å ³
Z	4
$D(\text{calcd})$	$2.74(5)$ g/cm ³
wavelength	Cu $K\alpha_1, \alpha_2$
2θ range	9.0 – 90.0°
time per step	420 s
2θ step size	0.02
no. of indep reflns	364
zero point	0.030(9)
Caglioti law parameters (U, V, W)	0, $-0.0072(8)$, 0
peak shape	pseudo-Voigt
background	Chebyshev polynomial, 12 coefficient
reliability factors	$R_p = 5.36$, $R_{wp} = 7.82$, $R_{exp} = 4.39$, GOF = 1.78
structure factor	$R_B = 3.59$

The crystal structure contains one crystallographically unique, six-coordinated V^{3+} atom, where the bond distances $\text{V}-\text{O}(\text{H})$ vary from 1.968(1) to 2.031(4) Å (average, 2.00 Å). BVS calculations²¹ of O(7) (calculated -1.08 ; expected -2) suggest the presence of a partial negative charge and a possible OH group, which support the structure model

Table 2. Atomic Coordinates and Isotropic Displacement Parameters for $\text{Na}_3\text{V}(\text{OH})(\text{HPO}_4)(\text{PO}_4)$

atom	Wyckoff	x	y	z	SOF ^a	B_{iso} (Å ²)
Na(1)	4	0	0.2287(3)	0	1	0.50(3)
Na(2)	4	0.1128(0)	0.5	0.7091(2)	1	1.96(1)
Na(3)	4	0.25	0.25	0.5	1	2.25(2)
V	4	0.25	0.25	0	1	1.27(3)
P(1)	4	0.3799(7)	0	0.7700(0)	1	0.738(9)
P(2)	4	0.1181(3)	0	0.6995(2)	1	2.76(0)
O(1)	4	0.4833(0)	0	0.7762(9)	1	0.502(6)
O(2)	4	0.3323(2)	0	0.5659(7)	1	2.53(2)
O(3)	8	0.3531(3)	0.1763(2)	0.8788(9)	1	1.83(1)
O(4)	8	0.1680(5)	0.1834(8)	0.7706(2)	1	2.95(9)
O(5)	4	0.0277(5)	0	0.7676(7)	1	3.11(6)
OH(6)	4	0.1183(9)	0	0.4677(5)	1	0.986(1)
OH(7)	4	0.2373(1)	0	0.1213(3)	1	0.500(2)

^a SOF = site occupancy factor.

adopted for the present refinement. The same calculations for the vanadium atom (see Table 3) gave a value of 3.02, which confirms the oxidation state 3+ determined by the magnetic measurements.

There are two crystallographically distinct phosphorus atoms, both with tetrahedral coordination. The lengths of the P(1)–O bonds range from 1.539(6) to 1.589(2) Å (average 1.571 Å) indicating some degree of multiple-bond character.

(21) Lufaso, M. W.; Woodward, P. M. *Acta Crystallogr., Sect. B* **2001**, *57*, 725.

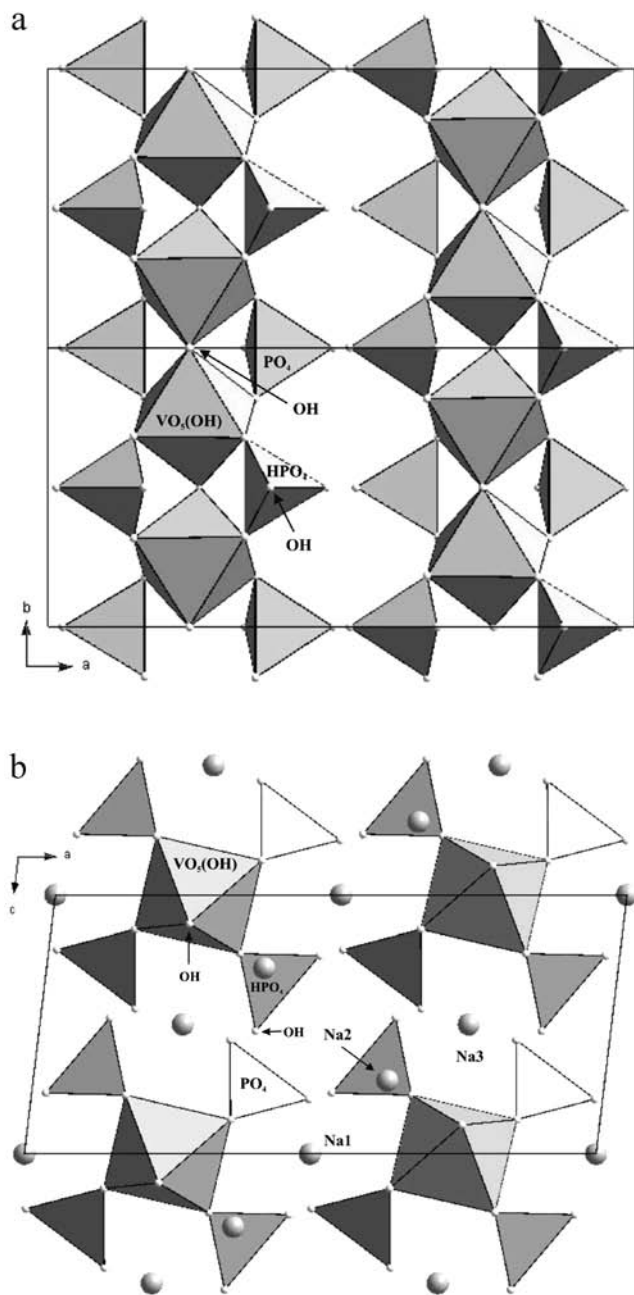


Figure 2. Structure of $\text{Na}_3\text{V}(\text{OH})(\text{HPO}_4)(\text{PO}_4)$ viewed along (a) [001] and (b) [010]. For clarity, the sodium atoms are omitted in part a.

The second phosphor tetrahedron is protonated, where the bond distances of $\text{P}(2)\text{--O}(\text{H})$ varies from 1.527(9) to 1.639(4) Å (average 1.588 Å). A longer distance of 1.639(4) Å is observed in the terminal bond $\text{P}(2)\text{--OH}(6)$, which indicates a partial negative charge. This was also confirmed by BVS calculations for the O(6) (calculated -1.189 ; expected -2). The absence of the valency value (Table 3) for P(1) and P(2) is around 9% and 14%, respectively. This can be attributed to a local disorder of the phosphorus atoms, which could not be modeled with the present set of data and requires further study on the first coordination sphere of the polyhedra.

The three distinct Na^+ cations show an irregular coordination geometry. They are coordinated with six (Na(1)), five (Na(2)), and eight (Na(3)) oxygen atoms, respectively. The

Table 3. Selected Bond Distances (Å) and BVSs (Σs) for $\text{Na}_3\text{V}(\text{OH})(\text{HPO}_4)(\text{PO}_4)$

Na(1)–O(5)	2× 2.412(7)	V–O(3)	2× 1.968(1)
Na(1)–O(3)	2× 2.425(7)	V–O(4)	2× 1.994(3)
Na(1)–O(1)	2× 2.524(3)	V–OH(7)	2× 2.031(4)
$\Sigma(\text{Na}(1)\text{--O}) = 1.041$		$\Sigma(\text{V--O}) = 3.02$	
Na(2)–O(1)	1× 2.107(1)	P(1)–O(2)	1× 1.539(6)
Na(2)–O(2)	1× 2.211(3)	P(1)–O(3)	2× 1.577(2)
Na(2)–OH(7)	1× 2.475(1)	P(1)–O(1)	1× 1.589(2)
Na(2)–O(4)	2× 2.477(4)	$\Sigma(\text{P}(1)\text{--O}) = 4.538$	
$\Sigma(\text{Na}(2)\text{--O}) = 1.257$		P(2)–O(5)	1× 1.527(9)
Na(3)–O(2)	2× 2.236(5)	P(2)–O(4)	2× 1.593(2)
Na(3)–O(4)	2× 2.463(0)	P(2)–OH(6)	1× 1.639(4)
Na(3)–OH(6)	2× 2.715(8)	$\Sigma(\text{P}(2)\text{--O}) = 4.346$	
Na(3)–O(3)	2× 2.997(8)		
$\Sigma(\text{Na}(3)\text{--O}) = 1.204$			

bond distances $\text{Na--O}(\text{H})$ vary from 2.107(1) to 2.997(8) Å with average distances of 2.454, 2.350, and 2.603 Å for Na(1), Na(2), and Na(3), respectively.

The presence of vanadium changes the metrics of the unit cell ($V = 788.3(9)$ Å³) when compared with the isostructural compounds containing Al ($V = 753.5(3)$ Å³) and Ga ($V = 774.8(6)$ Å³).¹⁸ The refined crystal structure shows that vanadium atoms occupy the octahedral site of Al/Ga; however, in contrast with the former, it can adopt different oxidation states. Considering that the ionic radii of six-coordinated vanadium in 4+ and 5+ oxidation states are smaller (0.58 and 0.54 Å, respectively) than the ones in 2+ and 3+ (0.79 and 0.64 Å, respectively),²² one of both valence states could be assumed. However, in order to get unambiguous information concerning the oxidation state of the vanadium ion, we performed magnetic measurements. Previous work on similar sodium vanadium phosphate compounds composed of chains of vanadium(IV) octahedra demonstrates the complexity of the cation distribution and vanadyl bond orientations in these materials.^{9,23} Such structural peculiarities can also be expected in the present compound considering the high isotropic displacement parameters of the sodium atoms. However, to reveal these features, high-resolution or single-crystal data are required.

3.3. Infrared Spectroscopy. The FTIR transmittance spectrum of $\text{Na}_3\text{V}(\text{OH})(\text{HPO}_4)(\text{PO}_4)$ is shown in Figure 3. It exhibits bands at 3587, 1156, 1066, 961, 882, 651, 556, and 467 cm^{-1} , and none of them could be assigned to amine vibration modes. The weak sharp band at 3587 cm^{-1} arises from the O–H bond stretching modes, supporting the suggestions from the Rietveld refinement. The asymmetric P–O stretching mode appears at 1156, 1066, 961, and 882 cm^{-1} , whereas the asymmetric O–P–O vibrations are observed at 651, 556, and 467 cm^{-1} .²⁴

3.4. Magnetic Properties. Figure 4 depicts the inverse magnetic susceptibility as a function of temperature, where a clear Curie–Weiss behavior was observed above 90 K. The paramagnetic effective moment $p_{\text{eff}} = 2.49 \mu_{\text{B}}/\text{V}$ is close to the theoretical value $2.83 \mu_{\text{B}}/\text{V}^{3+}$ (considering $g = 2$ and $S = 1$). The small deviation indicates a possible orbital

(22) Shannon, R. D. *Acta Crystallogr.* **1976**, A32, 751.

(23) Shpanchenko, R. V.; Dikarev, E. V.; Mironov, A. V.; Mudretsova, S. N.; Antipov, E. V. *J. Solid State Chem.* **2006**, 179, 2681.

(24) Gulians, V. V.; Benziger, J. B.; Sundaresan, S. *Chem. Mater.* **1995**, 7, 1485.

(25) Shpanchenko, R. V.; Mitiaev, A. S.; Chernaya, V. V.; Antipov, E. V.; Sakurai, H.; Muromachi, E. T. *J. Solid State Chem.* **2005**, 178, 3014.

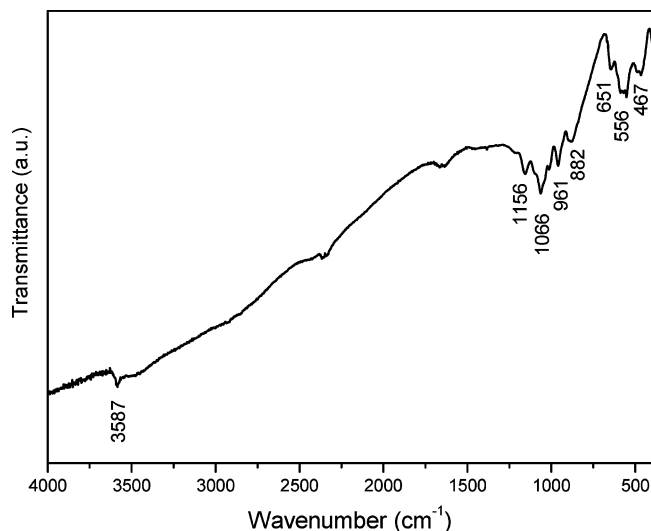


Figure 3. FTIR spectrum of $\text{Na}_3\text{V}(\text{OH})(\text{HPO}_4)(\text{PO}_4)$.

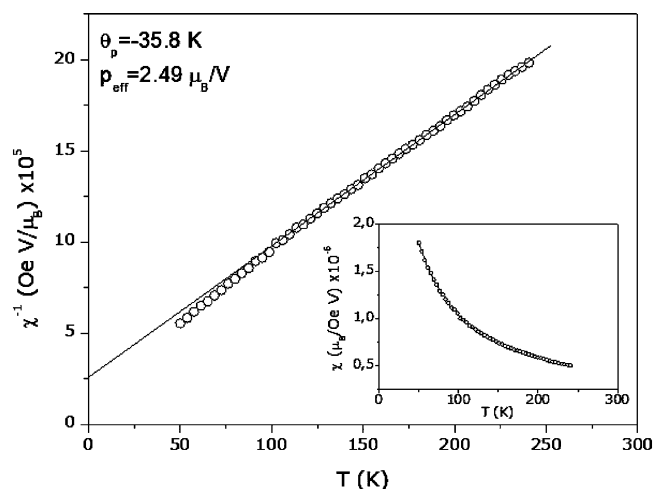


Figure 4. Inverse dc magnetic susceptibility as a function of the temperature. The paramagnetic effective moment is in accordance with isolated V^{3+} ions. The negative paramagnetic Curie temperature is a signature of the AFM arrangement of those V^{3+} ions, also in accordance with the V–O–V bridge angle of 127.3° (the crossover for vanadium compounds is 133° , above (below) which the system is FM (AFM)).²⁷ Inset: raw magnetic susceptibility.

contribution. This result ratifies our claim, based on an indirect conclusion from oxidation rules, that the vanadium ions in the present compounds have 3+ oxidation states. An experimental value of $2.61 \mu_{\text{B}}/\text{V}$ was found for another V^{3+} compound.²⁵ The negative paramagnetic Curie temperature ($\theta_{\text{p}} = -35.8 \text{ K}$) indicates an antiferromagnetic (AFM) arrangement between those V^{3+} ions. The exchange interaction between V^{3+} ions changes from AFM to ferromagnetic

(FM) when the V–O–V bridge angle reaches (increasing angle) a crossover value of 133° , as was already shown for some vanadium(III) complexes.²⁶ This fact is in accordance with the structural data, where the V–O–V angle is 127.3° .

On the other hand, we can expect some weak FM contribution, which, in fact, can be responsible for the deviation of the Curie–Weiss law below 90 K (Figure 4), where FM fluctuations of the magnetic interactions can exist. Indeed, it can arise as a result of (i) the tilting of the coordination polyhedra of V^{3+} (i.e., non-collinear alignment) and/or (ii) the obtained bridge angle V–O–V (127.3°), which is quite close to the crossover angle for AFM to FM arrangements. In this sense, a complete and deep analysis on the magnetic behavior of the present compound deserves attention and is in progress. The magnetic data presented here fit the scope of the present paper, determining therefore the oxidation state of the vanadium ions (V^{3+}) and their strongest magnetic arrangement (AFM).

4. Conclusion

A rare example of sodium vanadium(III) phosphate is synthesized by a hydrothermal method. This is the second metal phosphate prepared using MPMD. The crystal structure is determined by refinement of powder XRD data from atomic coordinates of the isotopic high-temperature- and high-pressure-obtained compound $\text{Na}_3\text{Al}(\text{OH})(\text{HPO}_4)(\text{PO}_4)$. The present compound is found to be the first sodium vanadium(III) phosphate containing isolated chains of vanadium polyhedra. From the magnetic measurements, it was possible to (i) confirm the 3+ oxidation state of the vanadium ions and (ii) determine the AFM arrangement between those ions through the chain.

Acknowledgment. The authors are thankful for financial support from FCT, POCI2010, and FEDER. S.F. also thanks FCT (SFRH/BPD/23771/2005) for a grant. The authors thank FCT for the VSM equipment (REEQ/1126/2001).

Supporting Information Available: Selected bond angles (Table S1), SEM images (Figure S1), TG curve (Figure S2), powder XRD pattern containing the absolute values of the collected intensity (Figure S3), and a CIF file. This material is available free of charge via the Internet at <http://pubs.acs.org>.

IC801318C

(26) Dean, N. S.; Mokry, L. M.; Bond, M. R.; O'Connor, C. J.; Carrano, C. J. *Inorg. Chem.* **1996**, *35*, 3541.

(27) Bond, M. R.; Czernuszewicz, R. S.; Dave, B. C.; Yan, Q.; Mohan, M.; Verastegue, R.; Carrano, C. J. *Inorg. Chem.* **1995**, *34*, 5857.